Balan, N., Yamamoto, M., Liu, J. Y., Otsuka, Y., Liu, H., Lühr, H. (2011): New aspects of thermospheric and ionospheric storms revealed by CHAMP. - Journal of Geophysical Research, 116, A07305

DOI: 10.1029/2010JA016399

New aspects of thermospheric and ionospheric storms revealed by CHAMP

N. Balan,[1,2,3] M. Yamamoto,[2] J. Y. Liu,[3] Y. Otsuka,[4] H. Liu,[2] and H. Lühr[5]

Received 23 December 2010; revised 23 March 2011; accepted 2 April 2011; published 8 July 2011.

[1] The neutral mass density N and electron density Ne at 400 km height measured by CHAMP during nine intense geomagnetic storms bring out some new aspects of the thermospheric and ionospheric storms. The thermospheric storms (increase of N) develop with the onset of the main phases (MP) of the geomagnetic storms and reach their peak phases before or by the end of the MPs. The ionospheric storms (change of Ne) in general undergo an initial negative phase (with the equatorial ionization anomaly (EIA) crests shifting poleward) before turning positive, and the positive storms reach their peak strengths (or phases) centered at ±25°–30° magnetic latitudes; in some (4) cases the positive storms develop without an initial negative phase and with the EIA crests shifting equatorward; in all cases the positive storms reach their peak phases before the end of the MPs and turn to conventional negative storms by the end of the MPs. The observations agree with the different aspects of a physical mechanism of the positive storms. The observations also reveal that the Halloween storms of 30 October 2003 with a short MP without fluctuations produced the strongest positive ionospheric storms through impulsive response, and there is strong equinoctial asymmetry in the ionosphere and thermosphere during geomagnetic storms.

Citation: Balan, N., M. Yamamoto, J. Y. Liu, Y. Otsuka, H. Liu, and H. Lühr (2011), New aspects of thermospheric and ionospheric storms revealed by CHAMP, *J. Geophys. Res.*, *116*, A07305, doi:10.1029/2010JA016399.

1. Introduction

[2] A series of rapid changes takes place in the global upper atmosphere and ionosphere following the onset of intense geomagnetic storms:

[3] 1. High latitude ionospheric electric fields promptly penetrate to low latitudes during the main phases (MP) of the storms [e.g., *Rastogi*, 1977; *Kikuchi et al.*, 1978]. The electric fields known as prompt penetration electric fields (PPEF) have eastward polarity in the dayside and westward polarity in the nightside [e.g., *Kelley et al.*, 2003]. The eastward PPEF enhances the net daytime eastward electric field over the equator [e.g., *Batista et al.*, 1991; *Fejer et al.*, 2007]. However, if the eastward PPEF occurs in the background of storm time disturbance dynamo electric fields (DDEF), which is westward during daytime [*Blanc and Richmond*, 1980], the net daytime electric field over the equator can be eastward or westward or null depending upon the strengths of the PPEF and DDEF [e.g., *Abdu et al.*, 2006]. The subauroral electric fields also intensifies and expands equatorward [e.g., *Foster*, 1993; *Heelis et al.*, 2009].

[4] 2. The high latitude thermosphere in both hemispheres gets heated. This expands the thermosphere, and causes storm time neutral winds to flow toward the equator in both hemispheres [e.g., *Roble et al.*, 1982], sometimes with an initial surge and traveling atmospheric disturbances (TADs) [e.g., *Prölss and Jung*, 1978; *Fuller-Rowell et al.*, 1994]. The expansion (and winds) changes the thermospheric composition to low O/N_2 ratio and high neutral mass density N [e.g, *Liu and Lühr*, 2005; *Sutton et al.*, 2005]; these are the chemical effects of the thermospheric expansion (and equatorward winds) [e.g., *Prölss*, 1995]. The equatorward winds (and TADs) also have mechanical effects (section 2). The thermospheric expansion, equatorward winds (and TADs) and their chemical and mechanical effects together can be called thermospheric storms.

[5] 3. The PPEF and thermospheric storms dramatically change the ionosphere (ionospheric storms), which affect all branches of telecommunication and navigation. The ionospheric storms are known to have a positive phase (or positive storms) followed by a long negative phase (or negative storms). The negative ionospheric storms in which the peak electron density Nmax (and electron density Ne and total electron content TEC) decreases much below its normal level causes serious problems (such as radio block outs) in ground-based HF radio communications. The negative storms therefore received much attention first when communications

[1]Control and Systems Engineering, University of Sheffield, Sheffield, UK.
[2]RISH, Kyoto University, Kyoto, Japan.
[3]Institute of Space Science, National Central University, Chung-Li, Taiwan.
[4]Solar-Terrestrial Environment Laboratory, Nagoya University, Nagoya, Japan.
[5]GFZ, German Research Centre for Geosciences, Potsdam, Germany.

0148-0227/11/2010JA016399

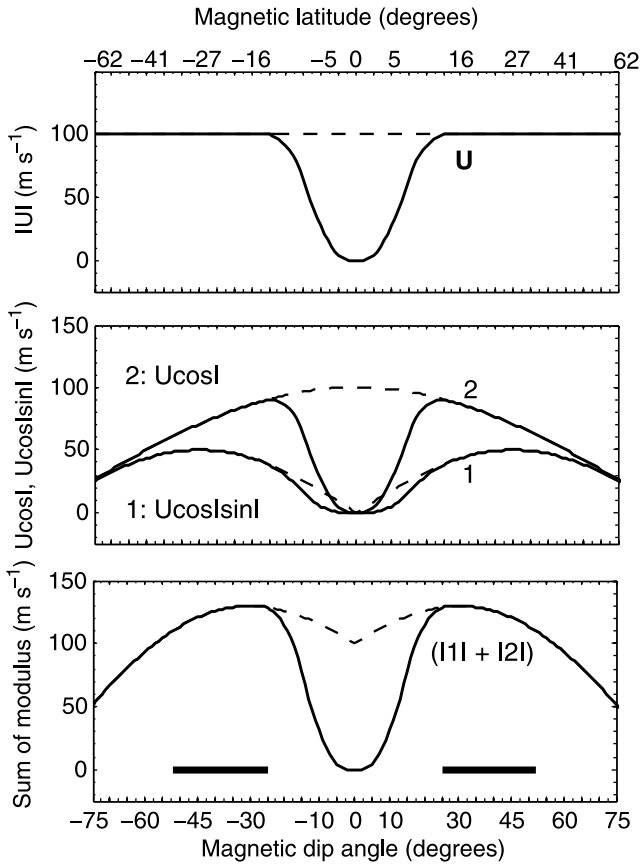

Figure 1a. (top) Latitude variations of the magnitudes of a typical (solid) and extreme (dashed) magnetic meridional equatorward neutral wind of velocity U, (middle) $U\cos I\sin I$ and $U\cos I$ for the two patterns of U, and (bottom) sum of the modulus of $U\cos I\sin I$ and $U\cos I$ for the two patterns of U; horizontal bars in Figure 1a (bottom) represent the latitude ranges of the possible positive ionospheric storm centers; direction of U is opposite in north and south.

depended mainly on HF radio, and the physical mechanisms of the negative storms are more or less understood [e.g., *Rishbeth*, 1991; *Prölss*, 1995; *Mendillo and Narvaez*, 2010].

[6] The positive ionospheric storms in which Ne, Nmax and TEC increase much above their normal levels can cause serious problems (such as time delay, range error and scintillations) in satellite communication and navigation. The positive storms have been studied by a number of scientists using observations and modeling [e.g., *Balan and Rao*, 1990; *Werner et al.*, 1999; *Sastri et al.*, 2000; *Basu et al.*, 2001; *Pincheira et al.*, 2002]. From these studies it has been known that the development of the positive storms involves electric fields and a mechanical effect of the equatorward neutral winds and TADs (height rise of the ionosphere) [e.g., *Prölss and Jung*, 1978]. Recently, *Kelley et al.* [2004] suggested that the root cause of the positive storms is the eastward PPEF that can enhance the daytime plasma fountain to a super fountain.

[7] However, modeling studies later showed that the PPEF, though enhances the plasma fountain to a super fountain and shifts the equatorial ionization anomaly (EIA) crests poleward, is unlikely to produce the positive storms because the PPEF accelerates the loss of ionization by diffusion [e.g., *Vijaya Lekshmi et al.*, 2007; *Balan et al.*, 2009]. The model results also showed that the mechanical effects of the equatorward winds alone can produce the positive storms [e.g., *Lu et al.*, 2008] with the EIA crests shifted equatorward [*Balan et al.*, 2009, Figure 6], and the mechanical effects of the winds and PPEF together also produce the positive storms [e.g., *Burns et al.*, 1995; *Lin et al.*, 2005].

[8] Recently a physical mechanism has been proposed to explain how the mechanical effects of the equatorward winds produce the positive ionospheric storms [*Balan et al.*, 2010]. The mechanism briefly reviewed and extended in section 2 has different aspects. However, most of the observations have supported mainly one aspect of the mechanism (PPEF and mechanical effects of the winds acting together) [e.g., *Mannucci et al.*, 2005; *Maruyama and Nakamura*, 2007]. In the present paper we use the CHAMP measurements of the electron density Ne and neutral mass density N [*Reigber et al.*, 2002] to study the developments of the ionospheric and thermospheric storms during 9 intense geomagnetic storms. The observations provide evidences for the different aspects of the mechanism of the positive ionospheric storms and bring out some new aspects. The model results supporting the different aspects of the mechanism are not repeated here because such results have been reported, and results referred.

[9] The positive ionospheric storms observed at subauroral latitudes [e.g., *Mendillo and Klobuchar*, 1975] have been interpreted in terms of the equatorward expansion of the convection electric fields, with no plasma transfer from low latitudes [e.g., *Foster*, 1993; *Heelis et al.*, 2009]. However, the mechanical effects of the equatorward winds can strengthen the positive storms at subauroral latitudes also. Recently, *Mendillo and Narvaez* [2010] reported detailed studies of the ionospheric storms at geophysically equivalent subauroral sites having comparable geographic and geomagnetic latitudes using the Nmax and hmax (peak height) data for 206 geomagnetic storms.

2. Physical Mechanism

[10] The physical mechanism of the positive ionospheric storms [*Balan et al.*, 2010] is briefly reviewed and extended here. The mechanism is applicable at low and mid latitudes in the presence of daytime production of ionization. It is illustrated using Figures 1a and 1b. Two patterns of the latitude variations of the effective horizontal magnetic meridional equatorward winds of velocity U are shown in Figure 1a (top); solid curve for a typical wind and dashed curve for an extreme wind. The wind of velocity U drives the ionospheric plasma up the field lines with a velocity $U\cos I$ of which the vertical component is $U\cos I\sin I$ with I being dip angle. The velocity $U\cos I\sin I$ raises the ionosphere to altitudes of reduced chemical loss and hence accumulates the plasma. Roughly, the ionospheric peak rises vertically by $\Delta h \approx (H_p/D_p)U\cos I\sin I$ where H_p is scale height and D_p is diffusion coefficient. This height rise can maximize at dip angles of ±45° as shown by the variations of $U\cos I\sin I$ in Figure 1a (middle, curves 1). Though the velocity component $U\cos I\sin I$ standing vertical on the inclined field line is

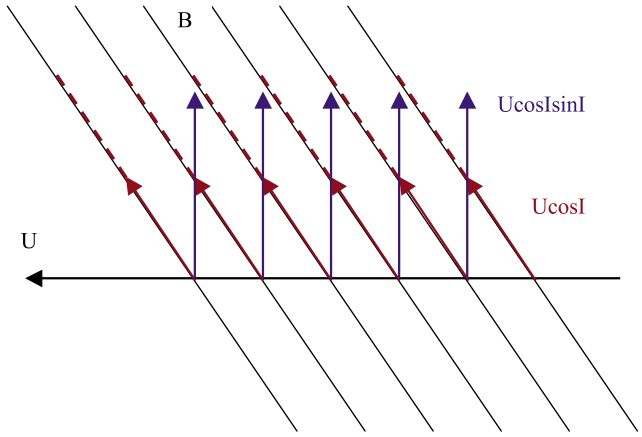

Figure 1b. A sketch illustrating the mechanical effects of neutral wind. A horizontal neutral wind of velocity U flowing equatorward through the inclined field lines raises the ionosphere by a velocity $U\cos I\sin I$. Though the component $U\cos I\sin I$ standing vertical in the inclined field line is unstable on its own (due to gravity), it is supported by the upward component $U\cos I$ along the field lines, like supporting a ball rolled up an inclined plane. In other words, the component $U\cos I$ supports the ionosphere at high altitudes and also reduces (or stops) the downward diffusion of plasma along the field lines (see text).

unstable on its own (due to gravity), it is supported by the component $U\cos I$ (Figure 1b). The slant component $U\cos I$ supports the vertical component $U\cos I\sin I$ (or supports the ionosphere at high altitudes), like supporting a ball rolled up an inclined plane.

[11] The downward plasma velocity along the field lines due to diffusion is $V_{\parallel} = -(D_p/n)(dn/dh + n/H_p)\sin I$ where n is plasma density [e.g., *Ratcliffe*, 1956]. The upward velocity component $U\cos I$ reduces (or stops) the downward diffusion of plasma along the field lines, and hence accumulates the plasma. This effect can maximize at low to equatorial latitudes as shown by curves 2 (Figure 1a, middle). The plasma gets accumulated centered at that latitude where the two mechanical effects optimize. As shown by the sum of the modulus of $U\cos I$ and $U\cos I\sin I$ (Figure 1a, bottom), the two mechanical effects together optimize centered at ±30° dip angles for the typical to extreme variations of the wind. The equatorward winds (and TADs) alone can therefore produce positive ionospheric storms centered at around ±30° dip angles (±16° magnetic latitudes).

[12] Strong eastward PPEFs on their own, though reduce the electron density through diffusion due to the $\mathbf{E} \times \mathbf{B}$ drift being inclined towards gravity, shift the EIA crests (in Nmax) up to ±35° magnetic latitudes [*Balan et al.*, 2009]. Therefore when the PPEFs and equatorward winds act together, the center of the positive storms can be in a range of latitudes depending upon their strengths. The horizontal bars in Figure 1a (bottom) give possible latitude ranges of the centers of the positive storms around noon, with the equatorward edges corresponding to the equatorward winds with no PPEF. When PPEFs and equatorward winds act together, the resulting positive storms can be narrow in latitudes due to the poleward compression of the plasma by the PPEFs (through plasma fountain) and equatorward compression of the plasma by the winds. Such positive storms can also have sharp peaks at the plasma converging points as observed [e.g., *Mannucci et al.*, 2005]. Also, since the downward diffusion velocity along the field lines is small around the equator, eastward PPEFs in the absence of equatorward winds can cause small increases in the density at the EIA crests as long as the crests are within about ±20° latitudes [e.g., *Huba et al.*, 2005].

[13] The positive ionospheric storms of varying strength and duration can occur in all seasons and at all levels of solar activity in the dayside (≈04–17 LT) longitudes of the main phase (MP) onset of the geomagnetic storms [e.g.,

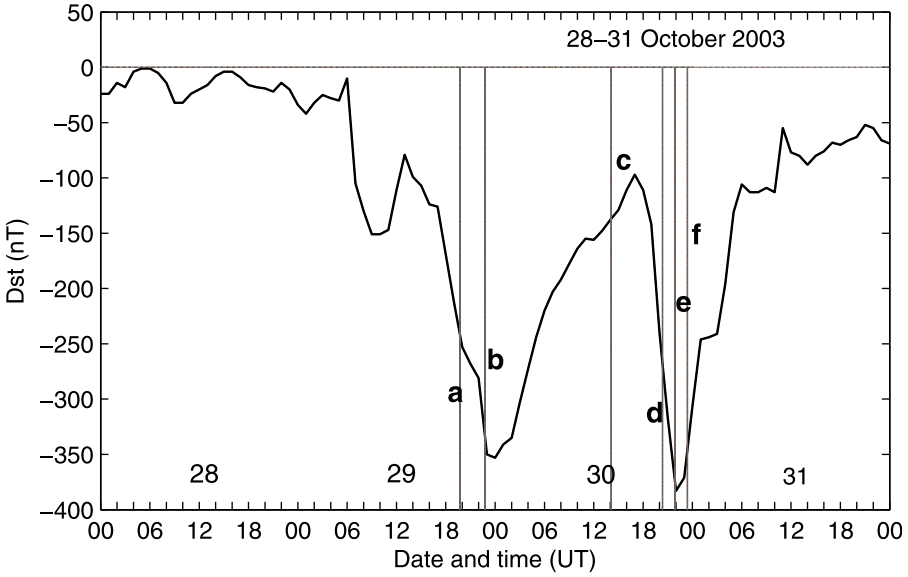

Figure 2a. The geomagnetic storms of 29–31 October 2003; vertical lines represent the times when CHAMP data are shown in Figures 2b and 2c.

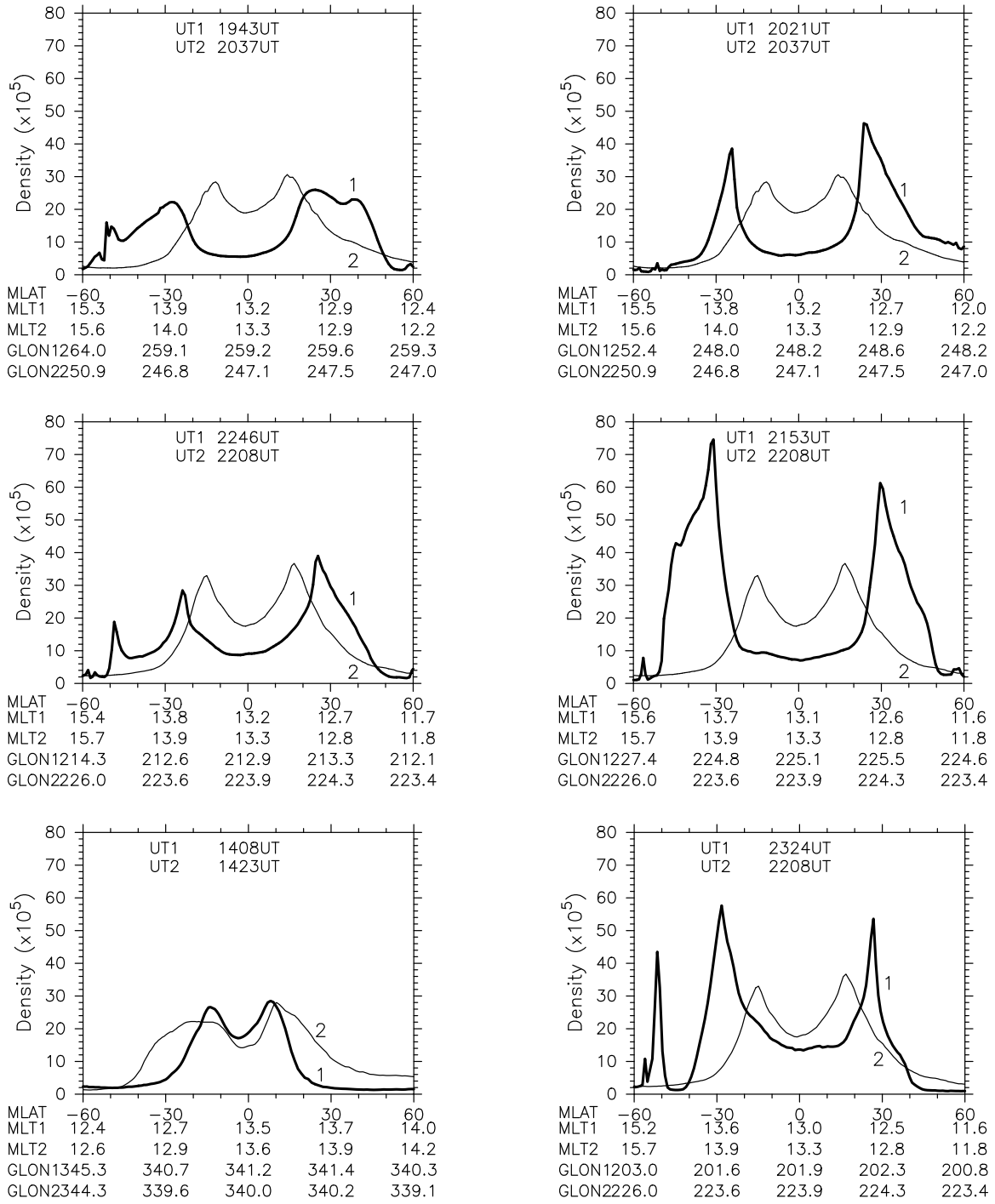

Figure 2b. Latitude variations of the electron density Ne at selected equatorial crossing times of CHAMP during the super storms of 29–30 October 2003 (thick curves 1) and at the corresponding times on the quiet day 28 October 2003 (thin curves 2).The satellite crossing times in UT (UT1 for storm and UT2 for quiet) are noted in the top of the blocks (indicated by the vertical lines in Figure 2a). The corresponding magnetic local times (MLT1 and MLT2) and geographic longitudes (GLOG1 and GLOG2) are noted in the bottom axes. Positive latitude is north.

Balan and Rao, 1990; *Prölss*, 1995]. Also, if the early part of the MP covers the afternoon (≈13–14 LT) hours of strong electron density, the resulting positive storms can be strong; the early part of the MP is important because the chemical effects of the winds can become dominant during the later part of the MP. For such geomagnetic storms, the ones with intense but short duration MPs without fluctuations can produce the strongest positive ionospheric storms through

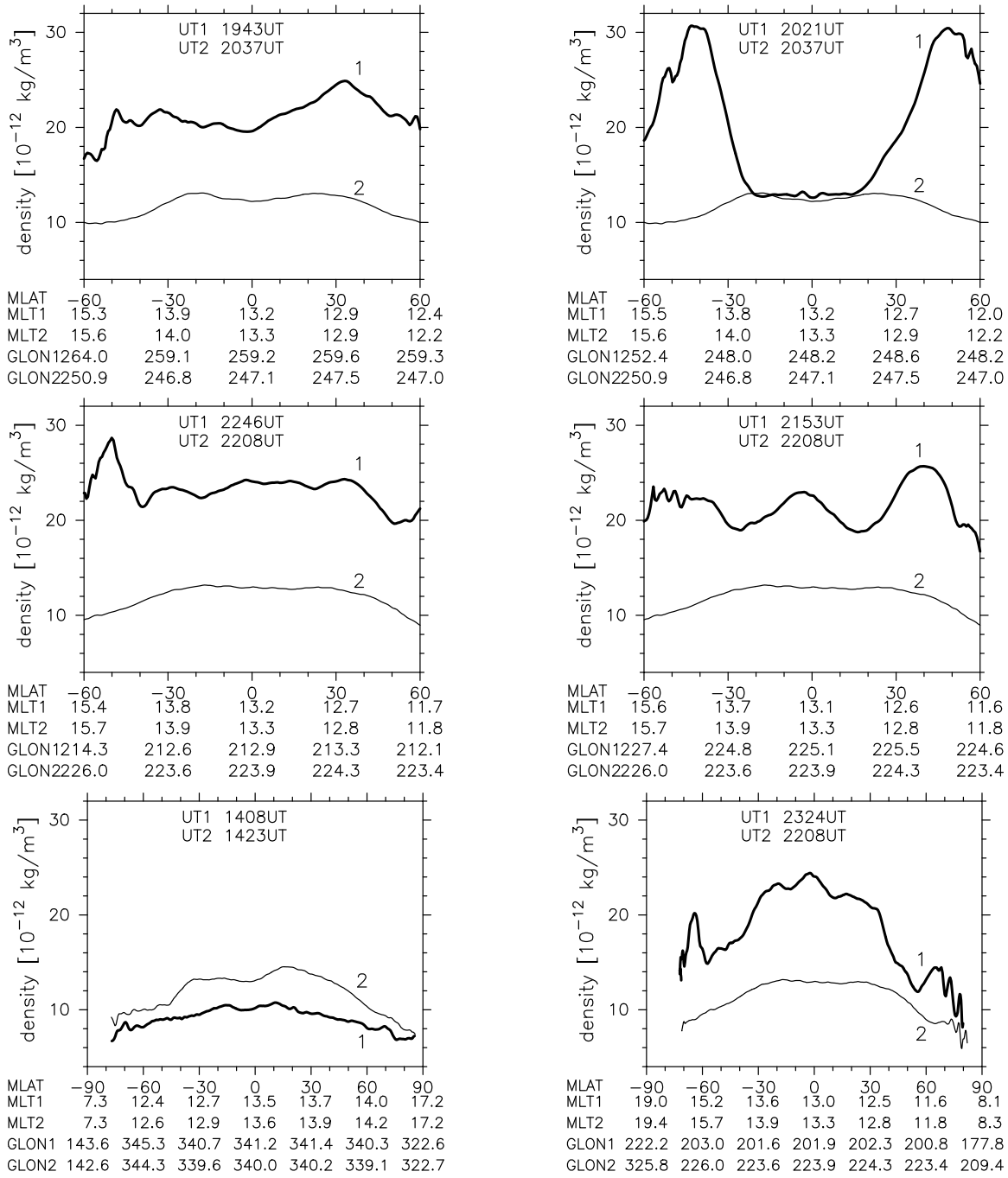

Figure 2c. Same as Figure 2b but for the neutral mass density N.

the impulsive response of the ionosphere and thermosphere (section 5).

3. CHAMP Data

[14] CHAMP (CHAllenging Mini-Satellite Payload) was launched on 15 July 2000 into a near-circular orbit with an inclination of 87.3°, an initial altitude of 456 km and orbital period of ≈90 minutes. The precession rate of its orbital plane is 1.5°/day. The in situ air mass density N is effectively probed by a triaxial accelerometer, which yields estimate of N with an accuracy of 10^{-14} kg m^{-3} at a sampling rate of 0.1 Hz (Level 2 data) [*Reigber et al.*, 2002]. The in situ electron density Ne is measured using a standard planar Langmuir probe (PLP) every 15 seconds. The data are normalized to 400 km height. The detailed procedure for deriving the data (N and Ne) and their normalization have been described by *Liu et al.* [2005]. Each satellite track varies by less than 5° in longitudes and 10 km in altitudes within ±60° latitudes; these variations do not affect the results obtained below.

[15] The CHAMP data (Ne and N) though limited to a single height (400 km) are good to investigate the thermospheric and ionospheric storms with and without strong

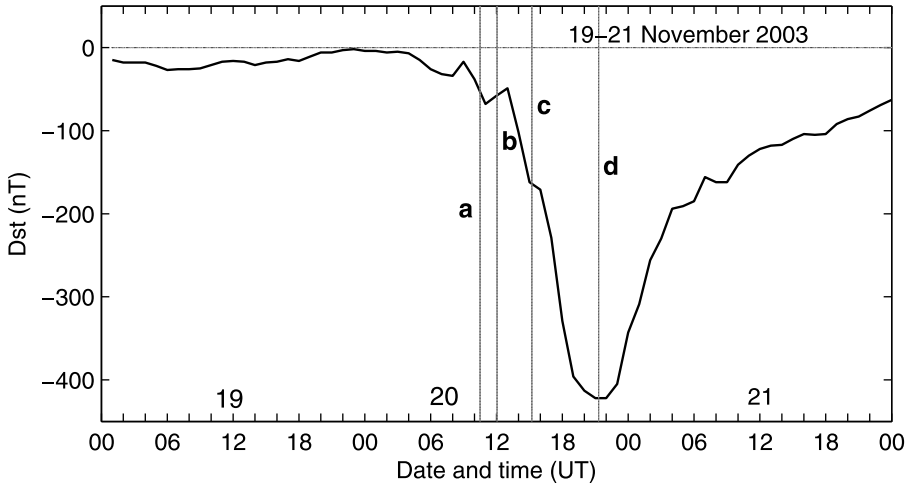

Figure 3a. The geomagnetic storm of 20 November 2003; vertical lines represent the times when CHAMP data are shown in Figures 3b and 3c.

electrodynamics. *Liu and Lühr* [2005] and *Sutton et al.* [2005] reported neutral density enhancements of up to 200%, 400% and 800% with respect to the quiet time values during the intense storms of 29 and 30 October 2003 and 20 November 2003, with large north-south difference. *Lei et al.* [2010] reported the neutral density increasing up to 400% during the main phases of the storms of 7–9 November 2004.

[16] The F region electric field (or PPEF) data are not available for the present storm periods. An alternative for the electric field is the storm time equatorial electrojet [e.g., *Balan et al.*, 2010]. However, the derivation of the electrojet requires the high resolution magnetic field data at equatorial and off equatorial locations in nearly same longitude, which are not available for the longitudes crossed by CHAMP during the MPs of the storms. But *Huang et al.* [2010] reported the vertical ion drift velocities over the equator measured by the DMSP F13 satellite at 18 LT during the intense storms on 31 March 2001 and 29–30 October 2003. The observations show strong upward ion velocities in the topside ionosphere during the MPs of all four storms, which are due to penetration, and downward ion velocities during the corresponding quiet periods. These DMSP data are used in the discussion of the effect of the PPEF in the present observations.

4. Observations

[17] As mentioned above, the CHAMP data (Ne and N) during 9 intense geomagnetic storms (Figures 1a and 2a for Dst), which include 4 reintensified storms, are analyzed. However, while Ne is available for all 9 storms, N is available only for 4 storms (one triple storm and one single storm). The main phases (MP) of the storms last from about 4 to 19 hours, and recovery phases (RP) last from 3 hours (due to reintensification) to over 24 hours. For each storm, the latitude variations of the CHAMP data (Figures 1a (middle) and 2b for Ne and Figures 1a (bottom) and 2c for N) at selected times during the storms (marked in Figures 1a and 2a) are compared with their variations at the corresponding times on previous quiet days. In Figures 2b, 2c, 3b, 3c, etc. storm time data are shown by thick curves (marked 1) and quiet time data by thin curves (marked 2). The equatorial crossing times of CHAMP in UT (UT1 for storm and UT2 for quiet) are given at the top of the images. The corresponding magnetic local times (MLT1 and MLT2) and geographic longitudes (GLOG1 and GLOG2) are noted in the bottom axes. The data on storm days and quiet days are for nearly same MLTs with a maximum difference of 45 minutes, which does not affect the results because the quiet time data vary little in 45 minutes. Below we briefly describe the observations, which will be discussed in section 5.

4.1. 29–30 October 2003

[18] A series of three geomagnetic storms occurred on 29–30 October 2003 (Figure 2a). The first storm has MP onset (MPO) at 07 UT and minimum Dst of –151 nT at 11 UT on 29 October (MP duration 4 hours). While this storm was about 3 hours into the RP a coronal mass ejection (CME) produced a super storm with MPO at 14 UT on 29 October and minimum Dst of −353 nT at 01 UT on 30 October (MP duration 11 hours). While this storm was 17 hours into RP another CME produced a second super storm with MPO at 18 UT and minimum Dst of −383 nT at 23 UT on 30 October (MP duration 5 hours).

4.1.1. Ionospheric Storms

[19] The CHAMP was crossing the 13.2 MLT meridian during the storms. The development of the ionospheric (and thermospheric) storms during the first (not so intense) geomagnetic storm (Figure 2a) is not described. Figure 2b shows the development of the ionospheric storms at selected times (marked in Figure 2a) during the following two super storms. The satellite crossed the first dayside MP (14–01 UT) in the 345°–180°E longitudes. Following the MP onset, Ne is found to decrease at all latitudes for about 4 hours with the EIA crests shifting poleward (data not shown), indicating the presence of an eastward PPEF. Soon the EIA crests shift further poleward to about ±28° with a large density reduction around the equator and with positive storms at around and poleward of the crests (Figure 2b, top left); this suggests the strengthening of the PPEF [e.g., *Huang et al.*, 2010] and

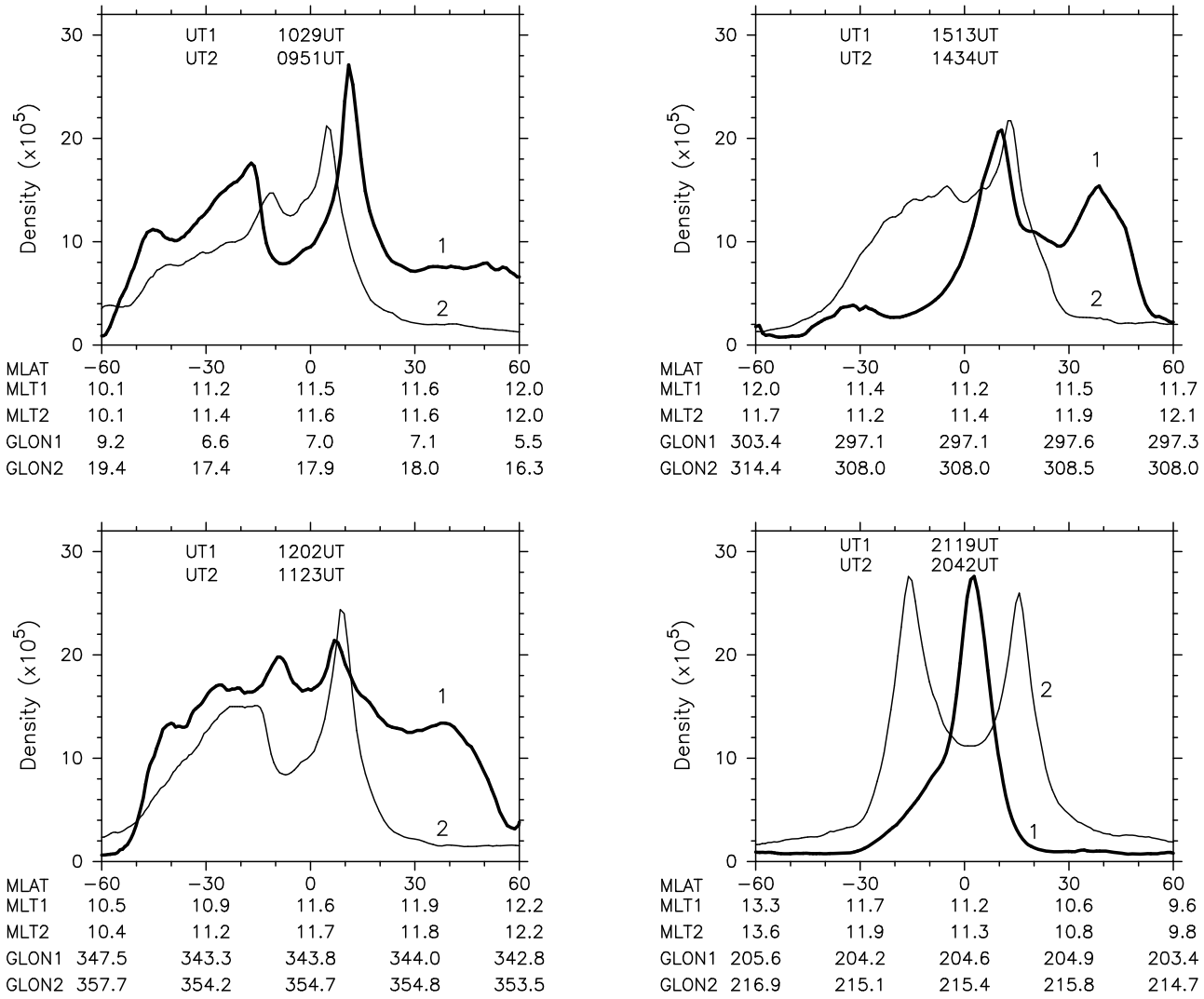

Figure 3b. Latitude variations of the electron density Ne at selected equatorial crossing times of CHAMP during the super storm of 20 November 2003 (thick curves 1) and at the corresponding times on the quiet day 19 November 2003 (thin curves 2). The satellite crossing times in UT (UT1 for storm and UT2 for quiet) are noted in the top of the blocks (indicated by the vertical lines in Figure 3a). The corresponding magnetic local times (MLT1 and MLT2) and geographic longitudes (GLOG1 and GLOG2) are noted in the bottom axes. Positive latitude is north.

action of the mechanical effects of the equatorward winds. The positive storms remain strong for another 2 hours. Then, about 2 hours before the end of the MP, the Ne at mid latitudes starts to decrease (Figure 2b, middle left) indicating the dominance of the chemical effects of the winds at these latitudes. By the end of the MP, the chemical effects produce conventional negative ionospheric storms at all latitudes (except around the equator), which become severe during RP. An example of the negative storm is shown in Figure 2b (bottom left); it corresponds to the late RP of the geomagnetic storm; such data are shown to discuss the corresponding neutral mass density variation during the RP.

[20] While the negative ionospheric storm was continuing, CHAMP crossed the next dayside MP (18–23 UT, Figure 2a) in the 285°–195°E longitudes. With the onset of the MP, sharp EIA crests quickly shift poleward (Figure 2b, top right). This suggests a strong eastward PPEF and mechanical effects of strong equatorward winds developing almost simultaneously. In the next orbit, the combined action of the strong PPEF [e.g., *Huang et al.*, 2010] and mechanical effects of the strong winds produces the strongest positive ionospheric storms centered at around ±30° magnetic latitudes (Figure 2b, middle right). By the end of the MP, the EIA crests start shifting equatorward with the density decreasing at all latitudes (Figure 2b, bottom right); this suggest the weakening of the PPEF and dominance of the chemical effect of the winds. Soon the chemical effects produce large negative ionospheric storms at all latitudes (data not shown). The signatures of secondary peaks (SEDs) poleward of the EIA crests [e.g., *Foster et al.*, 1993] can also be noted in Figure 2b (top left and middle right).

4.1.2. Thermospheric Storms

[21] The thermospheric storms (changes of N) during all geomagnetic storms are found to be similar. Figure 2c

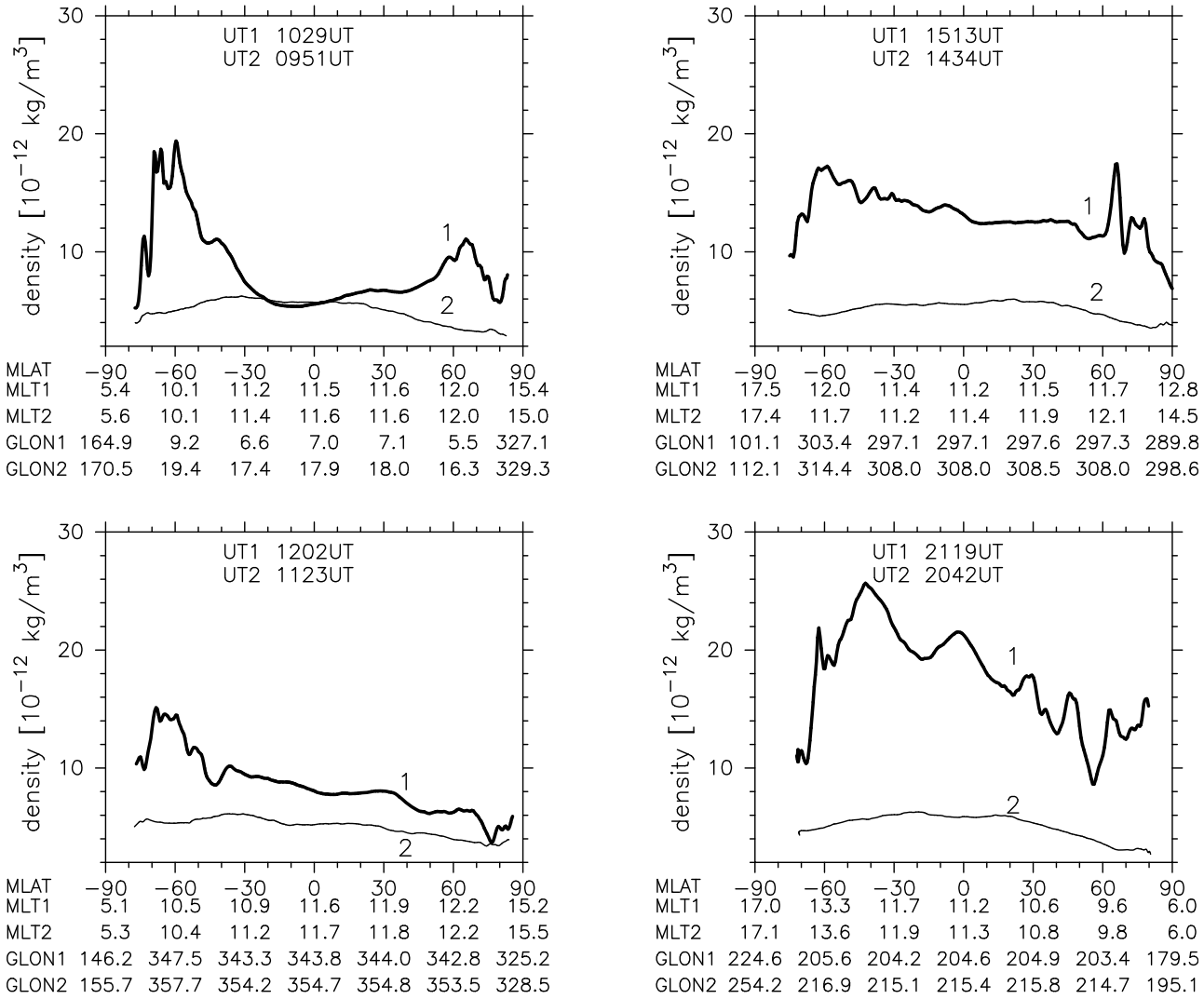

Figure 3c. Same as Figure 3b but for the neutral mass density N.

shows the latitude variations N during the two super storms at the times marked in Figure 2a (same as for Ne). At the onset of MP (at 14 LT), N has been slightly higher than normal due to the previous geomagnetic storm with very short RP (3 hours long). Over this high levels, N is found to increase first at high latitudes with the onset of the MP, which extends soon (in 1.5 hours) to low latitudes and gradually increases with time (Figure 2c, top left), and reaches peak levels by the end of MP (Figure 2c, middle left). During the RP, N gradually decreases, and reaches below its normal level (Figure 2c, bottom left) before recovering. The behavior of N during the second super storm is found to be similar but impulsive. N increases impulsively at high latitudes with the onset of MP (Figure 2c, top right), with no change at low latitudes. The increase of N from both hemispheres soon (in 1.5 hours) reach the equator (Figure 2c, middle right) when the latitude structure of N looks like a long-wave. By the end of the MP, N reaches its peak level over low latitudes while it decreases at higher latitudes (Figure 2c, bottom right). During RP, N is found to decrease much below its normal level before recovering. The temporal variations of N and Ne are discussed in section 5.

4.2. 19–20 November 2003

[22] An independent super storm occurred on 20 November 2003 (Figure 3a) with MPO at 03 UT. It reaches a minimum Dst of −422 nT at 22 UT giving an MP duration of 19 hours. Though it is most intense of all the storms, it has fluctuations (in Dst) for the first13 hours of the MP. CHAMP crossed the 11.5 MLT meridian during the MP with orbits in 100°-0°-210°E longitudes.

4.2.1. Ionospheric Storms

[23] Figure 3b shows the development of the ionospheric storms (in Ne). No significant changes in Ne are observed for about 3 hours after the onset of MP. Then a positive storm is found to start at mid and low latitudes, with the Ne around the equator decreasing and EIA crests shifting slightly poleward (Figure 3b, top left). This indicates the combined action of a weak eastward PPEF and mechanical effects of equatorward winds. Soon Ne increases at all latitudes including the equator and the EIA crests shift close to the equator (Figure 3b, bottom left), indicating the end of PPEF and strengthening of the mechanical effects of the winds. The peak phase of the positive storm (Figure 3b,

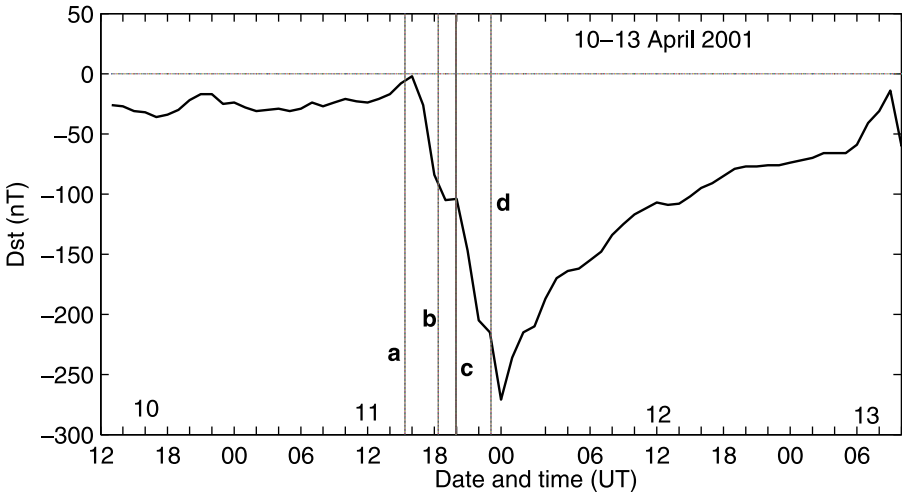

Figure 4a. The geomagnetic storm of 11–12 April 2001; vertical lines represent the times when CHAMP data are shown in Figure 4b.

bottom left) due to the winds alone is broad in latitudes (section 2). However, the positive storm is comparatively weak because the local time (11.5 MLT) is before noon and the equatorward winds are slow due to the fluctuating MP. While the positive storm continues in the winter (northern) hemisphere, a negative storm develops in the summer (southern) hemisphere (Figure 3b, top right) about 7 hours before the end of the MP. This agrees with the chemical effects of the equatorward winds acting earlier in the summer hemisphere [e.g., *Prölss*, 1995]. Before the end of the long MP, the chemical effects produce strong negative ionospheric storms in both hemispheres (Figure 3b, bottom right) except around the equator. The SED [*Foster*, 1993; *Heelis et al.*, 2009] might have also contributed to the positive storms in winter (Figure 3b top right).

4.2.2. Thermospheric Storms

[24] Figure 3c shows the thermospheric storms. A comparatively weak thermospheric storm (increase of N) starts at high latitudes with the onset of the long MP with fluctuations, and it does not extend to low latitudes for about 7 hours (Figure 3c, top right).With time the thermospheric storm extends to all latitudes (Figure 3b), and grows in strength (Figure 3c, top right), and reaches its peak level by the end of MP (Figure 3c, bottom right) with a large north-south asymmetry. During the RP, N is found to decrease to levels much below its normal level before recovering.

4.3. 11–12 April 2001

[25] Another independent super storm (Figure 4a) with MP onset (MPO) at around 16 UT and a minimum Dst of −271 nT at 24 UT (MP duration 8 hours) occurred on 11 April 2001 when CHAMP was crossing the 14 MLT meridian. The satellite had dayside orbits in the 315°-210°E longitudes during the MP. Before the MP onset, Ne shows almost the same latitude structure as on the previous quiet day (Figure 4b, top left). Following the MP onset (at 16 UT), a positive storm is found to develop gradually at mid latitudes with little changes at low latitudes (Figure 4b, bottom left). The storm grows to its peak level and extends to low latitudes with almost no change in the location of the EIA crests (compare Figures 4b bottom left and top left) well before the end of the MP. The storm then becomes weak (Figure 4b, bottom right), and turns negative (data not shown) by the end of the MP. These observations indicate the mechanical effects of the equatorward winds alone producing the broad positive storms with no PPEF in the longitudes of the satellite (section 2). However, the positive storm is comparatively weak, may be due to slow equatorward winds due to fluctuating MP.

4.4. 31 March 2001

[26] A super double geomagnetic storm (Figure 5a) occurred on 31 March 2001 with sudden commencement (SC) at 03 UT, MPO at 05 UT and minimum Dst of −387 nT at 09 UT (MP duration 4 hours). When the storm was about 8 hours into RP, it was reintensified with MPO at 17 UT and minimum Dst of −284 nT at 22 UT on the same day (MP duration 5 hours). CHAMP crossed the 15 MLT meridian with dayside orbits in the 165°–85°E longitudes during the first MP and 325°–250°E longitudes during the second MP.

[27] As shown by Figure 5b, following the MP onset Ne decreases in all latitudes (except at the EIA crest in the north) (Figure 5b, top left), which is found to continue for about 2 hours. Then a weak positive storm starts to develop at mid latitudes with the EIA crests shifting further poleward (Figure 5b, bottom left), which indicates the continuation of eastward PPEF [e.g., *Huang et al.*, 2010] and strengthening of the mechanical effects of the equatorward winds. The positive storm is found to reach its peak phase by the end of the short MP; simultaneously, a negative storm also develops at high latitudes (Figure 5b, top right). As time progressed in the RP, the negative storm becomes strong in the north with little changes in the south (Figure 5b, bottom right) indicating asymmetric thermospheric storms. During the reintensified super storm (Figure 5a), positive ionospheric storms are found to develop with no decrease of Ne around the equator and no poleward shift of the EIA crests (data not shown), indicating the mechanical effects of the equatorward winds alone producing the positive storms.

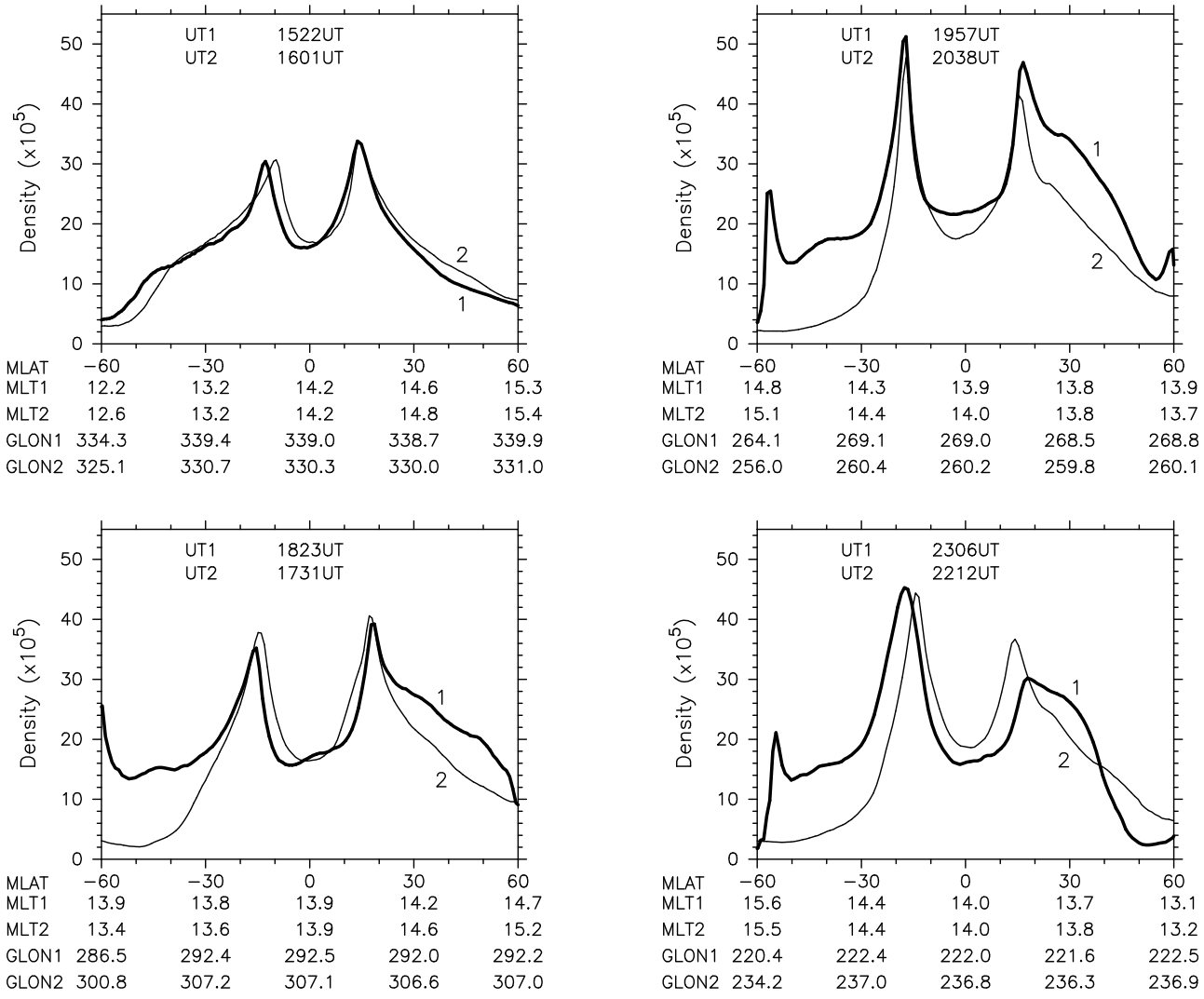

Figure 4b. Latitude variations of the electron density Ne at selected equatorial crossing times of CHAMP during the super storm of 11–12 April 2001 (thick curves 1) and at the corresponding times on the quiet day 10 April 2001 (thin curves 2). The satellite crossing times in UT (UT1 for storm and UT2 for quiet) are noted in the top of the blocks (indicated by the vertical lines in Figure 4a). The corresponding magnetic local times (MLT1 and MLT2) and geographic longitudes (GLOG1 and GLOG2) are noted in the bottom axes. Positive latitude is north.

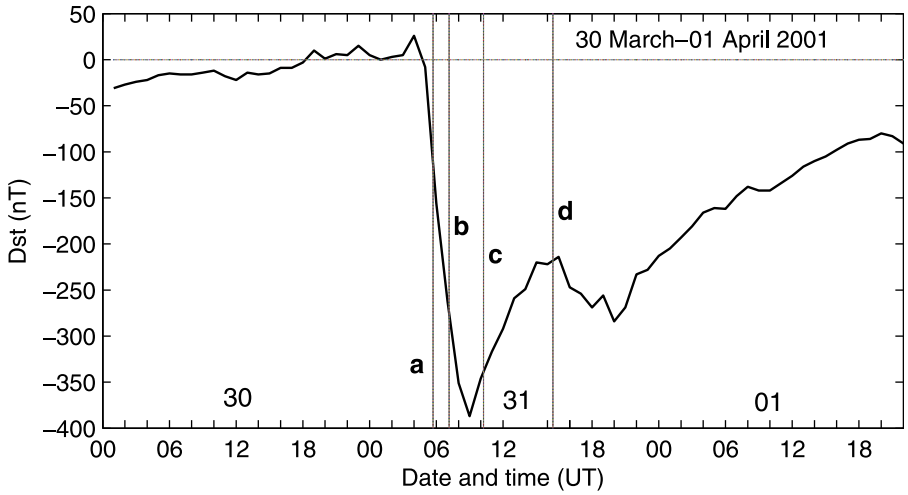

Figure 5a. The geomagnetic storms of 31 March 2001; vertical lines represent the times when CHAMP data are shown in Figure 5b.

4.5. 11–12 August 2000

[28] A double geomagnetic storm (Figure 6a) occurred on 10–12 August when CHAMP was crossing the 12 MLT meridian. The first storm was a moderate one (minimum Dst −106 nT). While it was recovering, a super storm occurred (minimum Dst −235 nT and MP duration 7 hours). During the MP of the first moderate storm (Figure 6a), Ne increases at and beyond the EIA crests (≈±20° latitudes) with no changes around the equator (Figure 6b, top left), indicating the mechanical effects of the winds alone producing the positive storms; the positive storm becomes weak with time (Figure 6b, bottom left) and turns into negative storms during the RP. During the intense geomagnetic storm (Figure 6a), CHAMP crossed the dayside MP in the 125°–200°E longitudes. Following the MP onset (at 03 UT), Ne increases in the winter (southern) hemisphere and around the equator with no changes in the summer hemisphere (Figure 6b, top right). This indicates asymmetric equatorward winds alone producing the positive ionospheric storms. During the early RP, the positive storm in the winter hemisphere becomes weak while a negative storm develops in the summer hemisphere (Figure 6b, bottom right).

5. Discussion

[29] The observations presented above show that the thermospheric storms undergo similar developments during all geomagnetic storms while the ionospheric storms show significant differences. The thermospheric storms (increase of N) originate at high latitudes with the onset of MPs, extend to cover equatorial latitudes (in 1.5 hours during intense MPs without fluctuations), grow to their peak phases before or by the end of the MPs and decay (N decreases) to normal levels during or by the end of the RP of the geomagnetic storms (data at selected times alone have been shown).

[30] However, the ionospheric storms in general undergo an initial negative phase for several hours (with the EIA crests shifting poleward) before turning positive; in 4 cases, broad positive storms develop without an initial negative phase and with the EIA crests shifting equatorward; in all cases, the positive storms reach their peak phases centered at ±15–30° magnetic latitudes before the end of the MPs; then they decay and turn to conventional negative storms by the ends of the MPs. The observations provide evidences for the different aspects of the physical mechanism of the positive ionospheric storms (section 2). The observations also indicate the contribution of the equatorward expansion of the subauroral electric fields on the positive storms at mid latitudes [e.g., *Foster*, 1993; *Heelis et al.*, 2009].

[31] The development of the thermospheric and ionospheric storms is illustrated further in Figures 7a and 7b for three intense geomagnetic storms; the timings are to be viewed with the uncertainty of the data (1.5 hours). Figure 7a shows the integrated storm time changes of Ne (thick solid curves) and N (dash-dotted curves) in the ±60° to ±20° magnetic latitude ranges during the MPs of the storms on 29–30 October 2003 and 20 November 2003; Figure 7b show the corresponding integrated storm time changes within ±20° magnetic latitude range (within EIA trough). The integrated storm time changes of Ne and N give the *sum of* (*storm* (*data*) *minus quiet* (*data*)) within the specified latitude ranges. Dst variation is also shown for the phase of the geomagnetic storms.

[32] As shown (Figures 7a and 7b), the integrated thermospheric storms on 29 and 30 October 2003 develop with the onset of the MPs in both latitude ranges apparently simultaneously indicating that the time of propagation from high to low latitudes is within 1.5 hours (the development on 30 October is from negative levels due to N being below normal during the previous RP, Figure 2c, bottom left). However, for the most intense and longest MP with fluctuations (20 November 2003), the thermospheric storms are weak for the first 10 hours and the storms reach low latitudes about 7 hours after their development at high latitudes. In all cases, the thermospheric storms reach their peak phases (at low latitudes) by the end of the MPs.

[33] The integrated ionospheric storms (Figures 7a and 7b) also develop with the onset of the MPs. The storms on 29 and 30 October undergo an initial negative phase at all latitudes before turning positive outside the trough region (the negative phase before MP onset is due to the negative

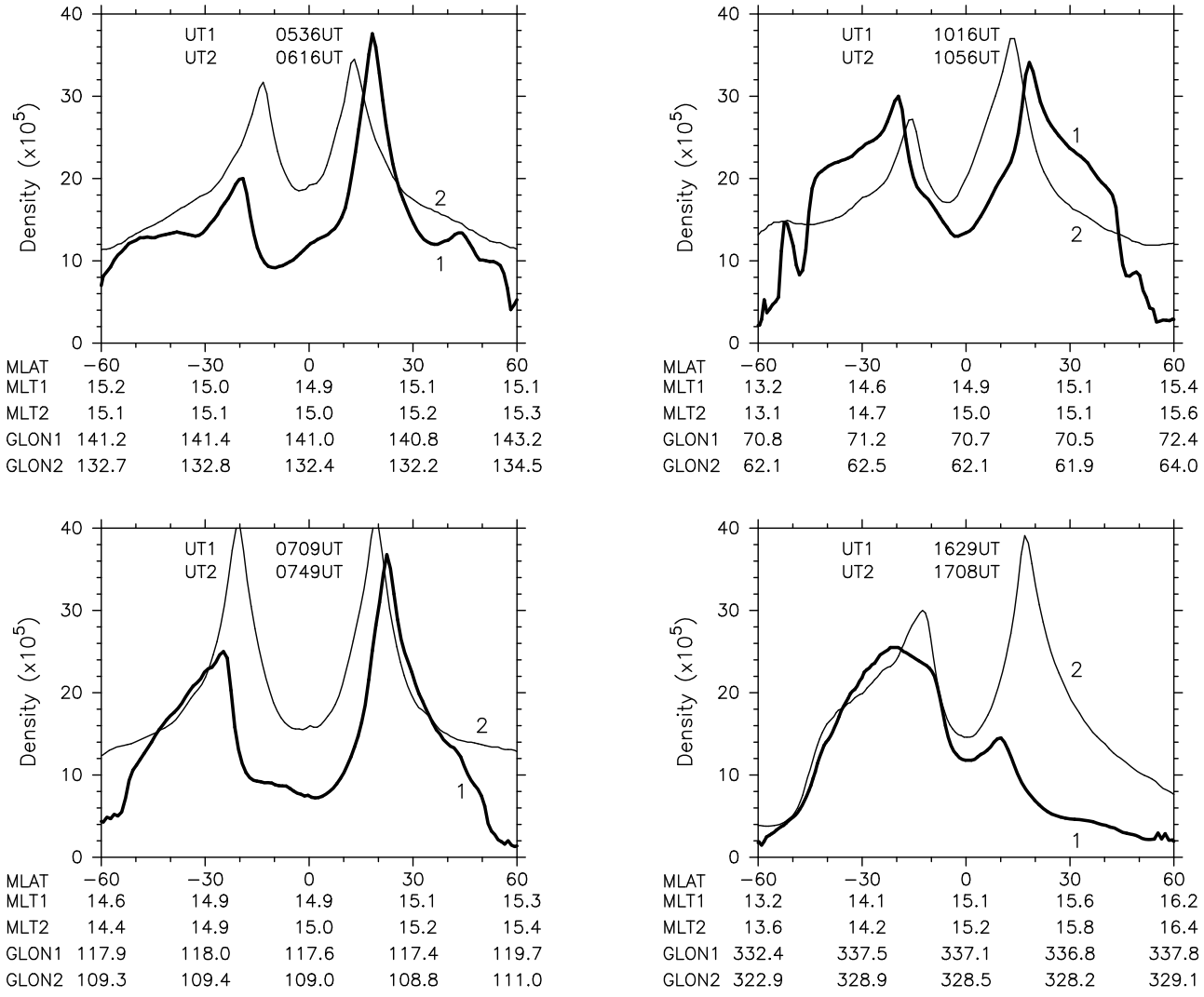

Figure 5b. Latitude variations of the electron density Ne at selected equatorial crossing times of CHAMP during the super storms of 31 March 2001 (thick curves 1) and at the corresponding times on the quiet day 30 March 2001 (thin curves 2). The satellite crossing times in UT (UT1 for storm and UT2 for quiet) are noted in the top of the blocks (indicated by the vertical lines in Figure 5a). The corresponding magnetic local times (MLT1 and MLT2) and geographic longitudes (GLOG1 and GLOG2) are noted in the bottom axes. Positive latitude is north.

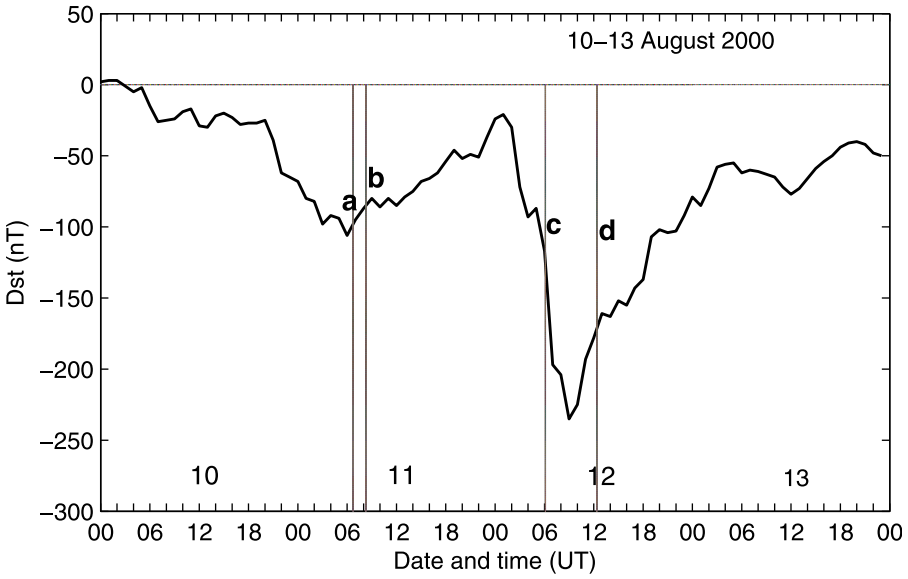

Figure 6a. The geomagnetic storms of 10–12 August 2000; vertical lines represent the times when CHAMP data are shown in Figure 6b.

storm during the previous RP); the positive storms reach their peak phases before the end of the MPs, and turn to conventional negative storms by the end of the MPs. However, the integrated negative storms within the trough (Figure 7b) continue to become most negative before or by the end of the MPs as expected from the action of eastward PPEF [*Balan et al.*, 2010]. However, on 20 November 2003, the integrated positive storms develop without an initial negative phase even inside the trough. These observations confirm that the (1) eastward PPEF produce the initial negative phase of the ionospheric storms, (2) mechanical effects of the equatorward winds alone or together with eastward PPEF produce the positive ionospheric storms, and (3) short MPs without fluctuations produce stronger ionospheric storms than long MPs with fluctuations.

[34] Of all the intense geomagnetic storms, the (Halloween) storm of 30 October 2003 with a short MP without fluctuations produced the strongest positive ionospheric storms (Figures 2b and 7a). This seems to be due to *impulsive response*. The high rate of energy input (not total energy input) at high latitudes during the short intense MP without fluctuations produces fast and strong equatorward surges and winds through an impulsive response of the thermosphere (Figure 2c, top right); the fast rate of change of Dst produces a fast growth of strong eastward PPEF (see the deepest and widest EIA trough, Figure 2b, top right and middle right); the two together produce the strongest positive ionospheric storms with sharp peaks at the converging points (section 2). This impulsive response is similar to the quiet time EIA becoming more symmetric and strong during the prereversal enhancement (PRE) of the eastward electric field than during other times of the day [*Balan and Bailey*, 1995]. It is also similar to the narrow but strongest daytime eastward PPEF on 09 November 2004 [*Fejer et al.*, 2007] producing the strongest F_3 layer ever recorded [e.g., *Balan et al.*, 2008].

[35] Another interesting difference is also noted in the ionospheric storms during the super storms on 31 March 2001 and 30 October 2003. Both super storms are equally intense (Dst = −383 nT and −387 nT) and have equally short MPs (5 hours) without fluctuations (Figures 2a and 5a); so impulsive response is expected in both cases. However, the positive storm on 31 March 2001 (Figure 5b) is weaker than that on 30 October 2003 (Figure 2b). The possible reasons include (1) weaker eastward PPEF in the longitudes (285°–195°E) crossed by CHAMP during the MP on 31 March than in the longitudes (165°–85°E) crossed during the MP on 30 October. Though F region electric field data are not available, *Huang et al.* [2010] show much weaker upward ion drift in the topside ionosphere on 31 March 2001 than on 30 October 2003. (2) Slower equatorward winds during the MP on 31 March (data not available) than on 30 October. These reasons seem to be possible because the two storms occurred at different equinoxes, and hence the thermosphere and ionosphere could have equinoctial asymmetries [e.g, *Balan et al.*, 1998]. (3) The two hours difference in the MLT sectors (13 MLT on 30 October and 15 MLT on 31 March) crossed by CHAMP during the two MPs could also contribute to the differences in the ionospheric storms. (4) Also, the storm on 31 March is independent and at higher solar activity (2001) while that on 31 October is reintensified and at lower solar activity (2003).

[36] The observations also show stronger north-south differences in Ne and N during geomagnetic storms than during quiet periods, which was reported by *Liu and Lühr* [2005] and *Sutton et al.* [2005]. As they discuss, the difference includes the seasonal asymmetry. The location of the geomagnetic poles in the two hemispheres can also contribute significantly to the asymmetry. In the same longitude, the equatorward winds and PPEF can be stronger in the hemisphere where the geomagnetic pole is closer to the (geographic) equator than in the opposite hemisphere.

[37] As mentioned in section 1, the positive ionospheric storms have been studied earlier using observations and models [e.g., *Werner et al.*, 1999; *Huba et al.*, 2005]. Some of the studies tried to interpret the positive storms in terms of the eastward PPEF [e.g., *Mannucci et al.*, 2005]. *Lin et al.*

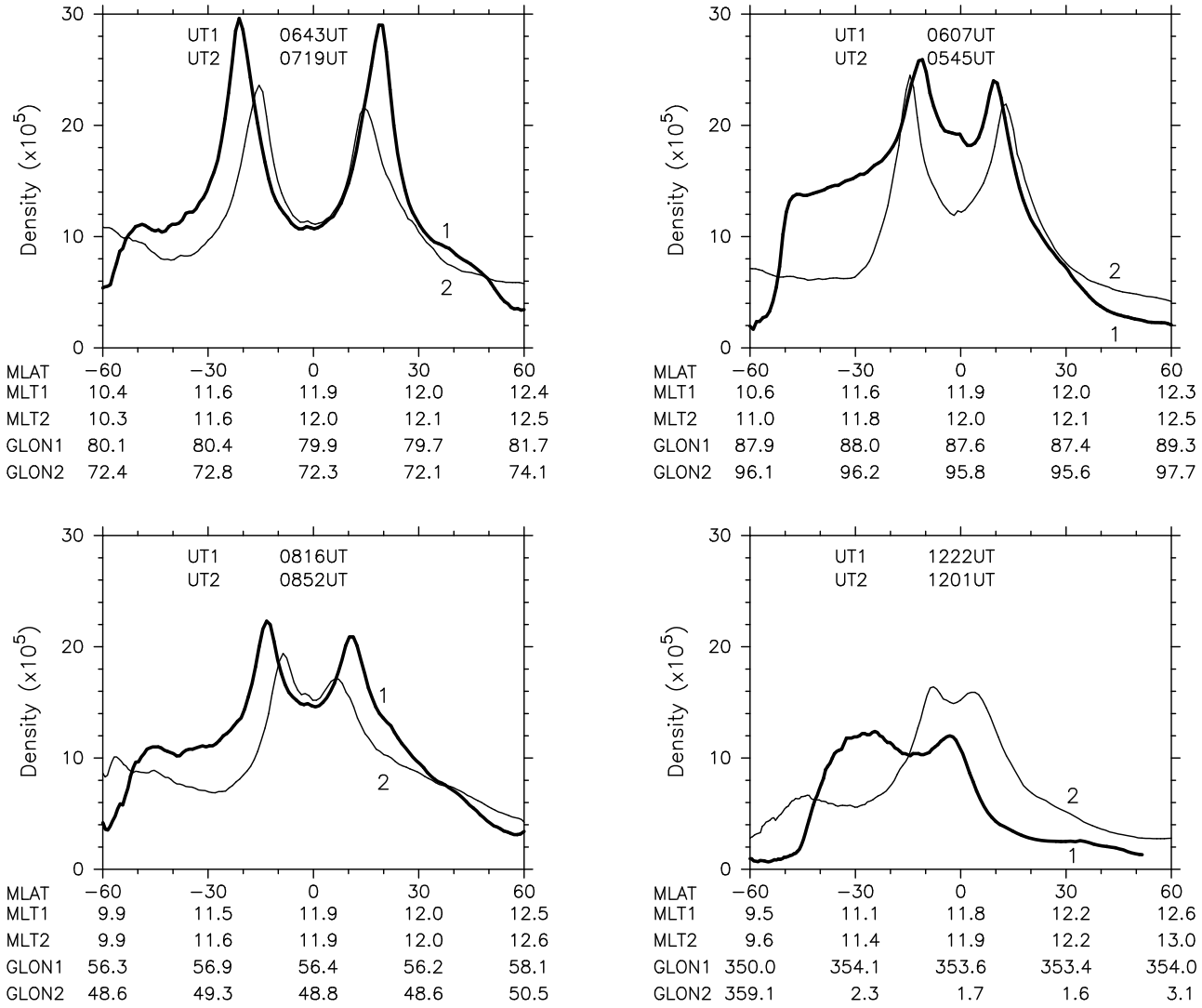

Figure 6b. Latitude variations of the electron density Ne at selected equatorial crossing times of CHAMP during the super storms of 10–12 August 2000 (thick curves 1) and at the corresponding times on the quiet day 9 August 2000 (thin curves 2). The satellite crossing times in UT (UT1 for storm and UT2 for quiet) are noted in the top of the blocks (indicated by the vertical lines in Figure 6a). The corresponding magnetic local times (MLT1 and MLT2) and geographic longitudes (GLOG1 and GLOG2) are noted in the bottom axes. Positive latitude is north.

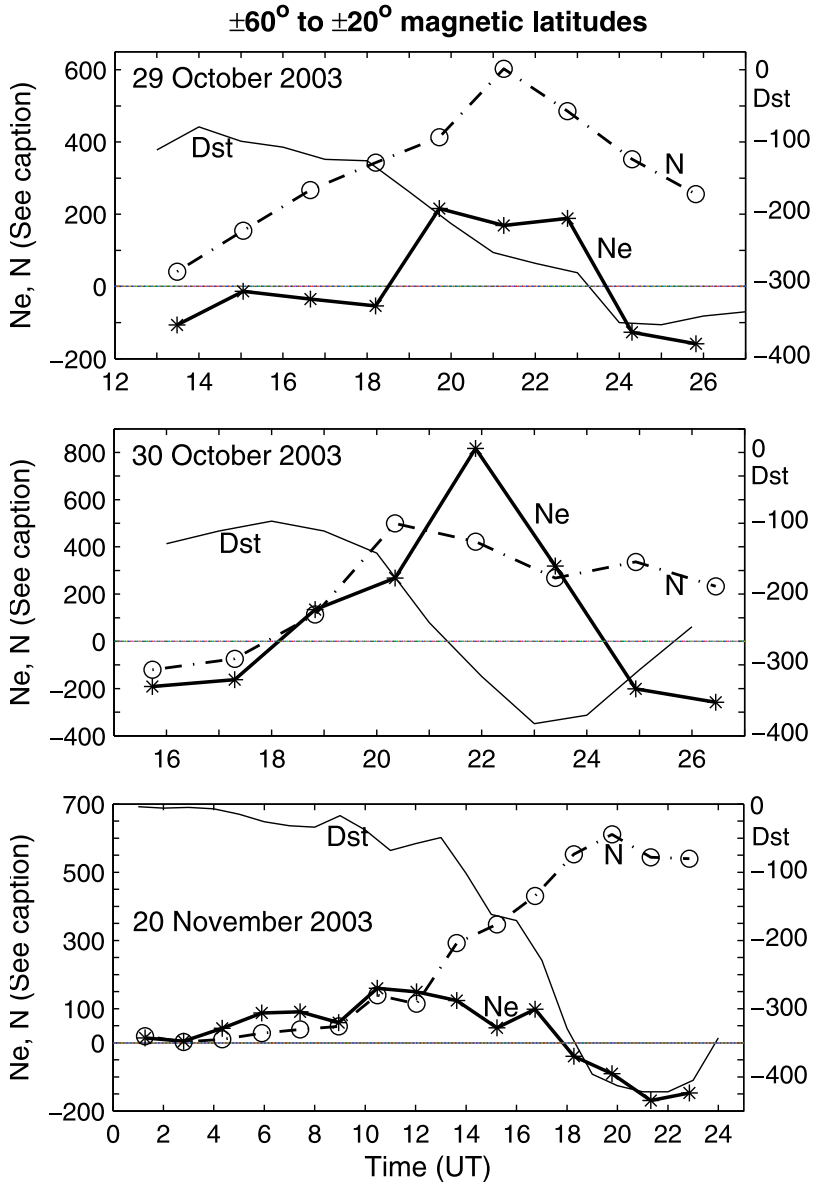

Figure 7a. The variations of the integrated storm time changes of Ne (thick solid curves) and N (dash-dotted curves) in the ±60° to ±20° magnetic latitude ranges during the main phases of the geomagnetic storms on (top) 29 October 2003, (middle) 30 October 2003, and (bottom) 20 November 2003. The integrated storm time changes of the data (Ne or N) gives the *sum of* (*storm* (*data*) *minus* (*quiet* (*data*)) within the specified latitude ranges. The units of Ne is in 10^5 cm^{-3} and of N is in 10^{12} kg m^{-3}. The Dst variation (thin curve) is also shown.

[2005] showed that in addition to PPEF, equatorward wind is important in producing the positive storms in Nmax and TEC. *Vijaya Lekshmi et al.* [2007] showed that the eastward PPEF on its own is unlikely to produce the positive ionospheric storms, and an equatorward wind is required to produce the positive storms. *Maruyama and Nakamura* [2007] suggested that disturbance dynamo electric field and storm time equatorward surge are important in expanding intense ionospheric storms to lower mid latitudes. Later *Lu et al.* [2008] showed that the primary cause of the positive ionospheric storms observed during the 10 September 2005 geomagnetic storm is the enhanced meridional wind rather than PPEF. *Balan et al.* [2009] showed that neutral wind alone can produce the positive storms. The CHAMP data in the present paper provide evidences for the different aspects of the physical mechanism of the positive storms (section 2), and bring out the impulsive response and equinoctial asymmetry of the thermosphere and ionosphere during geomagnetic storms.

6. Conclusions

[38] The CHAMP data (N and Ne) reveal some new aspects of the thermospheric and ionospheric storms. The

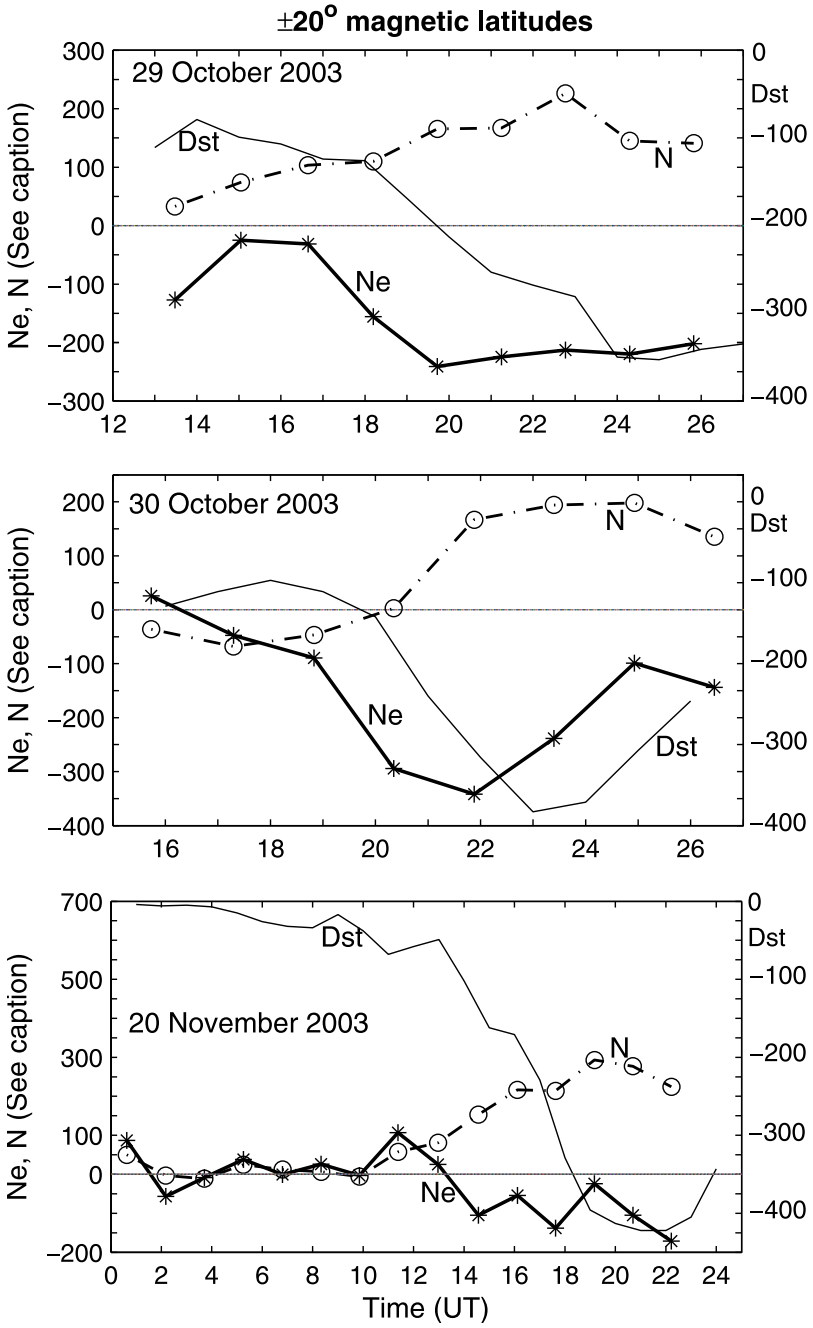

Figure 7b. Same as Figure 7a but for the ±20° magnetic latitude range.

thermospheric storms (increase of N) develop with the onset of main phases (MP) of the geomagnetic storms, and grow to their peak phases before or by the end of the MPs. The ionospheric storms (change of Ne) in general undergo an initial negative phase before turning positive; in some cases the ionospheric storms start positive without an initial negative phase; in all cases the positive storms reach their peak phases centered at ±15–30° magnetic latitudes before the end of MPs and turn to conventional negative storms by the end of the MPs. The observations provide evidences for the different aspects of a physical mechanism of the positive storms: The mechanical effects of the storm time equatorward neutral winds (and TADs) produce the positive storms (before their chemical effects become dominant) by reducing (or stopping) the downward diffusion of plasma along the field lines and by raising and supporting the ionosphere at high altitudes of reduced chemical loss. The winds (and TADs) and eastward PPEF together also produce the positive storms. However, the eastward PPEF on its own, though shifts the EIA crests to higher than normal latitudes, reduces Ne through diffusion due to the $\mathbf{E} \times \mathbf{B}$ drift being inclined towards gravity. The observations also reveal that the (Halloween) storms of 30 October 2003 produced the strongest positive ionospheric storms through impulsive response,

and there is strong equinoctial asymmetry and north-south asymmetry in the thermosphere and ionosphere during geomagnetic storms.

[39] **Acknowledgments.** N. Balan thanks RISH of Kyoto University (Japan) and the Institute of Space Science of National Central University (Taiwan) for providing visiting professor positions. The CHAMP was supported by the German Aerospace Center (DLR) in operation and by the Federal Ministry of Education and Research (BMBF) in data processing.

[40] Robert Lysak thanks Andrew Yau and another reviewer for their assistance in evaluating this paper.

References

Abdu, M. A., J. R. de Souza, J. H. A. Sobral, and I. S. Batista (2006), Magnetic storm associates disturbance dynamo effects over low and equatorial latitude ionosphere, in *Recurrent Magnetic Storms: Corotating Solar Wind Streams*, *Geophys. Monogr. Ser.*, vol. 167, edited by B. Tsurutani et al., pp. 283–304, AGU, Washington, D. C.

Balan, N., and G. J. Bailey (1995), Equatorial plasma fountain and its effects – possibility of an additional layer, *J. Geophys. Res.*, *100*, 21,421–21,432.

Balan, N., and P. B. Rao (1990), Dependence of ionospheric response on the local time of sudden commencement and intensity of storms, *J. Atoms. Terr. Phys.*, *52*, 269–275.

Balan, N., Y. Otsuka, G. J. Bailey, and S. Fukao (1998), Equinoctial asymmetries in the ionosphere and thermosphere observed by the MU radar, *J. Geophys. Res.*, *103*, 9481–9495.

Balan, N., S. V. Thampi, K. Lynn, Y. Otsuka, H. Alleyne, S. Watanabe, M. A. Abdu, and B. G. Fejer (2008), F3 layer during penetration electric field, *J. Geophys. Res.*, *113*, A00A07, doi:10.1029/2008JA013206.

Balan, N., H. Alleyne, Y. Otsuka, D. Vijaya Lekshmi, B. G. Fejer, and I. McCrea (2009), Relative effects of electric field and neutral wind on positive ionospheric storms, *Earth Planets Space*, *60*, 1–7.

Balan, N., K. Shiokawa, Y. Otsuka, T. Kikuchi, D. Vijaya Lekshmi, S. Kawamura, M. Yamamoto, and G. J. Bailey (2010), A physical mechanism of positive ionospheric storms at low and mid latitudes through observations and modeling, *J. Geophys. Res.*, *115*, A02304, doi:10.1029/2009JA014515.

Basu, S., Sa. Basu, K. M. Groves, H. C. Yeh, F. J. Rich, P. J. Sultan, and M. J. Keskinen (2001), Response of the equatorial ionosphere in the South Atlantic region to the great magnetic storm of July 15, 2000, *Geophys. Res. Lett.*, *28*, 3577–3580.

Batista, I. S., E. de Paula, M. A. Abdu, N. Trivedi, and M. Greenspan (1991), Ionospheric effects of the March 13, 1989, magnetic storm at low and equatorial latitudes, *J. Geophys. Res.*, *96*, 13,943–13,952.

Blanc, M., and A. Richmond (1980), The ionospheric disturbance dynamo, *J. Geophys. Res.*, *85*, 1669–1686.

Burns, A. G., T. L. Killeen, W. Deng, G. R. Carignan, and R. G. Roble (1995), Geomagnetic storm effects in the low- to middle-latitude upper thermosphere, *J. Geophys. Res.*, *100*, 14,673–14,691.

Fejer, B. G., J. W. Jensen, T. Kikuchi, M. A. Abdu, and J. L. Chau (2007), Equatorial ionospheric electric fields during the November 2004 magnetic storm, *J. Geophys. Res.*, *112*, A10304, doi:10.1029/2007JA012376.

Foster, J. C. (1993), Storm-time plasma transport at middle and high latitudes, *J. Geophys. Res.*, *98*, 1675–1689.

Fuller-Rowell, T. J., M. V. Codrescu, R. J. Moffett, and S. Quegan (1994), Response of the thermosphere and ionosphere to geomagnetic storms, *J. Geophys. Res.*, *99*, 3893–3914.

Heelis, R. A., J. J. Sojka, M. David, and R. W. Schunk (2009), Storm time density enhancements in the mid latitude dayside ionosphere, *J. Geophys. Res.*, *114*, A03315, doi:10.1029/2008JA013690.

Huang, C. S., F. J. Rich, and W. J. Burke (2010), Storm time electric fields in the equatorial ionosphere near the dusk meridian, *J. Geophys. Res.*, *115*, A08313, doi:10.1029/2009JA015150.

Huba, J. D., G. Joice, S. Sazykin, R. Wolf, and R. Spiro (2005), Simulation study of penetration electric field effects on the low- to mid-latitude ionosphere, *Geophys. Res. Lett.*, *32*, L23101, doi:10.1029/2005GL024162.

Kelley, M. C., J. J. Makela, J. L. Chau, and M. J. Nicolls (2003), Penetration of the solar wind electric field into the magnetosphere/ionosphere system, *Geophys. Res. Lett.*, *30*(4), 1158, doi:10.1029/2002GL016321.

Kelley, M. C., M. N. Vlasov, J. C. Foster, and A. J. Coster (2004), A quantitative explanation for the phenomenon known as storm-enhanced density, *Geophys. Res. Lett.*, *31*, L19809, doi:10.1029/2004GL020875.

Kikuchi, T., T. Araki, H. Maeda, and K. Maekawa (1978), Transmission of polar electric fields to the equator, *Nature*, *273*, 650–651.

Lin, C. H., A. D. Richmond, R. A. Heelis, G. J. Bailey, G. Lu, J. Y. Liu, H. C. Yeh, and S. Y. Su (2005), Theoretical study of the low and mid-latitude ionospheric electron density enhancement during the October 2003 superstorm: Relative importance of the neutral wind and the electric field, *J. Geophys. Res.*, *110*, A12312, doi:10.1029/2005JA011304.

Lei, J., J. P. Thayer, A. G. Burns, G. Lu, and Y. Deng (2010), Wind and temperature effects on thermosphere mass density response to the November 2004 geomagnetic storm, *J. Geophys. Res.*, *115*, A05303, doi:10.1029/2009JA014754.

Liu, H., and H. Lühr (2005), Strong disturbance of the thermospheric density due to storms: CHAMP observations, *J. Geophys. Res.*, *110*, A09S29, doi:10.1029/2004JA010908.

Liu, H., H. Lühr, V. Henize, and W. Köhler (2005), Global distribution of the thermospheric density derived from CHAMP, *J. Geophys. Res.*, *110*, A04301, doi:10.1029/2004JA010741.

Lu, G., L. P. Goncharenko, A. D. Richmond, R. G. Roble, and N. Aponte (2008), A dayside ionospheric positive storm phase driven by neutral winds, *J. Geophys. Res.*, *113*, A08304, doi:10.1029/2007JA012895.

Mannucci, A. J., B. T. Tsurutani, B. A. Iijima, A. Komjathy, A. Saito, W. D. Gonzalez, F. L. Guarnieri, J. U. Kozyra, and R. Skoug (2005), Dayside global ionospheric response to the major interplanetary events of October 29–30, 2003 "Halloween Storms", *Geophys. Res. Lett.*, *32*, L12S02, doi:10.1029/2004GL021467.

Maruyama, T., and M. Nakamura (2007), Conditions for intense ionospheric storms expanding to lower mid latitudes, *J. Geophys. Res.*, *112*, A05310, doi:10.1029/2006JA012226.

Mendillo, M., and J. Klobuchar (1975), Investigations of the ionospheric *F* region using multistation total electron content observations, *J. Geophys. Res.*, *80*, 643–650.

Mendillo, M., and C. Narvaez (2010), Ionospheric storms at geophysically-equivalent sites – Part 2: Local time storm patterns for sub-auroral ionospheres, *Ann. Geophys.*, *28*, 1449–1462.

Pincheira, X. T., M. A. Abdu, I. S. Batista, and P. G. Richards (2002), An investigation of ionospheric responses, and disturbance thermospheric winds, during magnetic storms over South America sector, *J. Geophys. Res.*, *107*(A11), 1379, doi:10.1029/2001JA000263.

Prölss, G. W. (1995), Ionospheric *F* region storms, in *Handbook of Atmospheric Electrodynamics*, edited by H. Volland, pp. 195–248, CRC Press, Boca Raton, Fla.

Prölss, G. W., and M. J. Jung (1978), Traveling atmospheric disturbances as a possible explanation for daytime positive storm effects of moderate duration at middle latitudes, *J. Atmos. Terr. Phys.*, *40*, 1351–1354.

Rastogi, R. G. (1977), Geomagnetic storms and electric fields in the equatorial ionosphere, *Nature*, *268*, 422–424.

Ratcliffe, J. A. (1956), The formation of ionospheric layers F_1 and F_2, *J. Atmos. Terr. Phys.*, *8*, 260–269.

Reigber, C., H. Lühr, and P. Schwintzer (2002), CHAMP mission status, *Adv. Space Res.*, *30*, 129–134.

Rishbeth, H. (1991), *F*-region storms and thermospheric dynamics, *J. Geomag. Geoelectr.*, *43*, 513–524.

Roble, R. G., R. E. Dickinson, and E. C. Ridley (1982), Global circulation and temperature structures of thermosphere with high-latitude plasma convection, *J. Geophys. Res.*, *87*, 1599–1614.

Sastri, J., N. Jyoti, V. Somayajulu, H. Chandra, and C. Devasia (2000), Ionospheric storm of early November 1993 in the Indian equatorial region, *J. Geophys. Res.*, *105*, 18,443–18,455.

Sutton, E. K., J. M. Forbes, and R. S. Nerem (2005), Global thermospheric neutral density and wind response to the severe 2003 geomagnetic storms from CHAMP accelerometer data, *J. Geophys. Res.*, *110*, A09S40, doi:10.1029/2004JA010985.

Vijaya Lekshmi, D., N. Balan, V. K. Vaidyan, H. Alleyne, and G. J. Bailey (2007), Response of the ionosphere to super geomagnetic storms: Observations and modeling, *Adv. Space Res.*, *41*, 548–555, doi:/10.1016/j.asr.2007.08.029.

Werner, S., R. Bauske, and G. W. Prölss (1999), On the origin of positive ionospheric storms, *Adv. Space. Res.*, *24*, 1485–1489.

N. Balan, Control and Systems Engineering, University of Sheffield, Sheffield S10 3JD, UK. (b.nanan@sheffield.ac.uk)

H. Liu and M. Yamamoto, RISH, Kyoto University, Kyoto 611-0011, Japan.

J. Y. Liu, Institute of Space Science, National Central University, Chung-Li 32001, Taiwan.

H. Lühr, GFZ, German Research Centre for Geosciences, Potsdam D-14473, Germany.

Y. Otsuka, Solar-Terrestrial Environment Laboratory, Nagoya University, Nagoya 464-8601, Japan.